Phenomena Affecting the Interferometric Determination of Concentration Profiles of Micromolecules Diffusing Along a Stiff-Chain Polymer Film

D. F. STAMATIALIS, M. SANOPOULOU, J. H. PETROPOULOS

Physical Chemistry Institute, Demokritos National Research Centre, GR-15310 Aghia Paraskevi, Athens, Greece

Received 17 July 1996; accepted 30 December 1996

ABSTRACT: A detailed examination of the interferometric determination of penetrant concentration profiles during longitudinal penetration of micromolecular liquids in glassy polymer films, nonrigidly clamped between glass plates, is presented. Penetration of methylene chloride and methyl alcohol (representing strong and relatively weak swelling agents, respectively) into cellulose acetate films, characterized, respectively, by a degree of acetylation of 2.45 (CA-2.45) and 2.0 (CA-2.0) acetyl groups per monomer unit, was studied, and the importance of certain factors, which should be taken into account in order to obtain reliable concentration profiles, is demonstrated. In particular, conversion of the interferometrically determined optical path difference profiles to concentration profiles requires taking account of (i) the deviation from linearity of the refractive index–concentration relation, due to the filling of the excess free volume of the polymer by the penetrant and (ii) swelling of the clamped polymer film in the thickness direction, with particular attention to deviations from uniform specimen thickness. In the example of strong swelling agent penetration (CA-2.45/MC), no detectable increase in film thickness over that of the original dry film was detected, as a result of the fact that the polymer becomes sufficiently plasticized to deform plastically along the penetration axis under the clamping pressure. During weak swelling agent penetration (CA-2.0/MA), on the other hand, significant swelling in the thickness direction was observed, because the polymer is less plasticised and can undergo plastic deformation as above only to a limited extent. In this case, it is important to guard against deviations from uniform specimen thickness. The relevant strain birefringence profiles provided significant information which helped to establish the above picture. The calculated concentration profiles are discussed in the light of the measured penetration kinetics and in relation to the magnitude of the clamping pressure. © 1997 John Wiley & Sons, Inc. J Appl Polym Sci **65:** 317–327, 1997

Key words: cellulose acetate, transport of liquid penetrants in films of; interferometry; refractive index vs. concentration relation; swelling of the membrane in the thickness direction; concentration profiles

INTRODUCTION

Many years ago, the technique of studying unidimensional micromolecular transport in a polymeric medium by immersing a polymer film clamped between glass plates in a liquid penetrant (see Fig. 1) was successfully demonstrated.[1–4] The main advantage of this technique is that the propagation of the penetrant in a given direction X along the polymer film and the corresponding swelling of the polymer can be followed *in situ*. In particular, one can study penetration

Correspondence to: M. Sanopoulou.

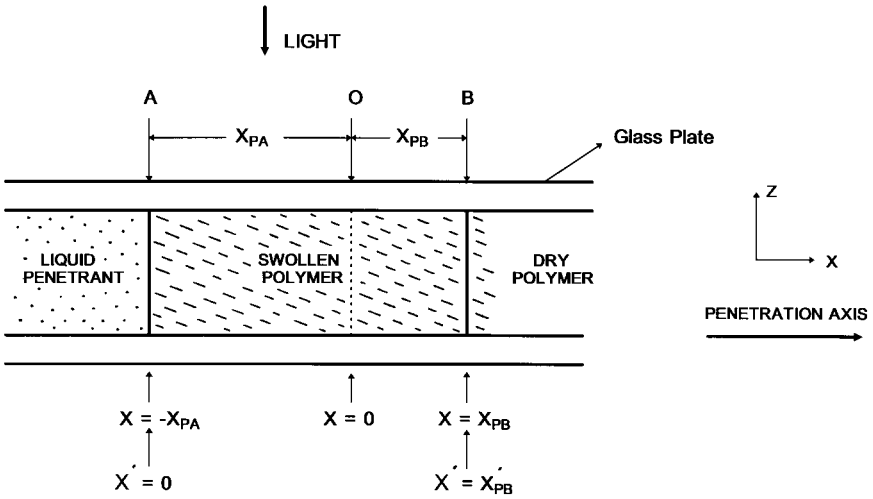

Figure 1 Schematic side view representation of unidimensional penetration of a liquid swelling agent into a polymer film sandwiched between glass plates. O: original position of the edge of the film; A: position of film edge (swelling front) at time t; B: position of visible penetrant front at time t.

and swelling kinetics by observing the propagation of visible penetration and swelling fronts through a microscope, while information about the profile of penetrant concentration C and of the accompanying structural relaxation of the polymer along the axis of penetration can be obtained simultaneously by means of suitable optical methods, namely, microinterferometry and polarizing microscopy, respectively.[5,6]

Interferometry usually involves measurement of fringe displacements Δy, which correspond to optical path length differences (OPDs), between a location $X' > 0$ along the axis of penetration on the film specimen and a reference location, usually chosen within the pure liquid penetrant adjoining the edge of the film, which is located at $X' = 0$ (see Fig. 1). Given the geometrical path length in each case, namely, $l(X')$ and l_L, respectively, and the refractive index of the pure liquid penetrant n_L, the refractive index profile of the swelling polymer film $n(X')$ follows from the relation

$$\Delta y(X') = n(X')l(X') - n_L l_L \qquad (1)$$

In the absence of significant changes in volume upon mixing the polymer with the liquid penetrant, n is expected to vary linearly with the concentration of penetrant in the polymer, C (expressed in mol per unit vol of the swollen polymer), i.e., $dn/dC = \text{const.}$[5,6] Then, if the swelling film specimen is constrained by the glass plates to a uniform thickness, i.e.:

$$l_L = l(X') = l_0 \qquad (2)$$

(where l_0 denotes thickness of the completely dry polymer region), the penetrant concentration profile is given by

$$\frac{C(X')}{c_L} = \frac{n(X') - n_P}{n_L - n_P} = 1 - \frac{\Delta y(X')}{\Delta y_0} \qquad (3a,b)$$

where eq. (3b) follows from eq. (1). In eq. (3a), n_P is the refractive index of the pure polymer and $c_L = 1/\bar{V}_L$, where $\bar{V}_L$ is the molar volume of the pure liquid penetrant. In eq. (3b), Δy_0 is the OPD in the completely dry polymer region.

The simple relation between $C(X')$ and $\Delta y(X')$ given by eqs. (3) may be expected to be applicable to rubbery polymers, where the $n(C)$ relation is generally at least approximately linear and the suppression of thickness swelling in the constrained film specimen is readily made up by a corresponding increase in longitudinal swelling.

This is no longer so in the case of glassy polymers. Here, on the one hand, substantial deviations from the linear $n(C)$ relation may occur at low C, due to the presence of "excess free volume" (which is also responsible for the well-known general tendency of these polymers to swell at low C less than expected on the basis of volume additivity of polymer and liquid penetrant upon mixing).[3,7–9] Under these circumstances, eq. (3a) obviously breaks down and one must resort to direct determination of the $n(C)$ relation (at least in

the lower concentration region), in order to claim reliable conversion of the $n(X')$ to the $C(X')$ profile.

On the other hand, the uniform specimen thickness condition,[2] on which eq. (3b) is based, can always be imposed, in principle, by clamping the glassy polymer film sufficiently rigidly to suppress swelling along the thickness direction.[3] However, this is likely to entail a marked modification of the sorption and transport behavior, in relation to what would have been observed in the absence of such extreme constraint. In practice, the imposition of some constraint in the thickness direction is, of course, unavoidable, in order to ensure firm contact (and thus prevent liquid penetration) between the film specimen and the glass plates. Once complete suppression of thickness swelling is no longer an objective, however, it is best to use spring clips as the clamping device, in order to maintain an approximately constant known force on the glass plates.[5,6] Then, if the swelling polymer is sufficiently plasticized, it will tend to deform plastically in the direction of penetration under the clamping pressure. If the swelling polymer is only weakly plasticized, the swelling pressure developed may be sufficient to push the glass plates apart, thus allowing a limited amount of dilation in the thickness direction. It is obviously necessary to establish that eq. (2) and, hence, eq. (3b), remain valid under these conditions. If this is not so, it becomes necessary to devise means of correcting the OPD profile for the resulting variation in specimen thickness $\Delta l(X') = l(X') - l_0$, in order to deduce the refractive index profile. The swelling behavior observed may be further affected by the fact that swelling deformation in the $-X$ direction may be hindered significantly by friction between the surfaces of the swelling polymer and the glass plates (which will also be dependent on clamping pressure).

In the present article, we report OPD profiles pertaining to the transport of methylene chloride (MC) and methyl alcohol (MA) along nonrigidly clamped cellulose acetate films, coupled with data on the swelling of these films in the thickness direction, as well as on the variation of the refractive index with penetrant concentration. These data provide a good demonstration of the precautions which should be taken in order to derive reliable penetrant distribution profiles in nonrigidly clamped films penetrated by strong or relatively weak swelling agents, respectively. The results obtained are discussed in the light of supplementary strain birefringence profiles and penetration rate data and in relation to the magnitude of the clamping pressure.

EXPERIMENTAL

Materials

Cellulose acetate (CA-2.45) powder of 39.8% acetyl content (ca. 2.45 acetyl groups per glucose monomer unit) was supplied by Eastman Chemicals (code name E398-30) with the following specifications: melting range 230–250°C; T_g = 189°C; viscosity (measured according to ASTM D-871 [Formula A] and D-1343) = 114 poise (30 s).

Films of dry thickness l_P = 50–120 μm (measured with a mechanical feeler gauge reading to 1 μm) were prepared by casting a 20% solution of the above polymer in acetone (prefiltered through a G4 sintered glass filter) on a clean glass surface. The solution was spread with a knife blade moving on rails and loosely covered to ensure subsequent slow solvent evaporation in an atmosphere partially saturated with acetone vapor. Solvent evaporation was completed in the open atmosphere and then *in vacuo.* These films were used for the experiments with MC. The equilibrium swelling ratio of the free film observed upon immersion in the liquid was 9.3 : 1, as compared with 1.4 : 1 when swollen in MA.

The experiments with MA were carried out on films of somewhat lower acetyl content to enhance the uptake of this penetrant. For this purpose, the above films were partially hydrolyzed to an acetyl group content of 2.0 per glucose monomer unit (CA-2.0), in a 40% aqueous solution of acetic acid, in the presence of H_2SO_4 as a catalyst, (pH 0–1) at 25°C, then washed in distilled water for 3 days to remove residues of the reagents, dried in an oven at 70°C for 3 days, and finally evacuated for 10 days. The degree of acetylation of the membrane was determined by titration (involving complete hydrolysis to cellulose with excess of 0.2*N* NaOH solution followed by back titration of excess NaOH with standard 0.1*N* oxalic acid[10]). The swelling ratio observed, upon equilibration with liquid MA, was 1.5 : 1 for the free film.

Both CA-2.45 and CA-2.0 films tended to swell to a greater extent in the direction of the thickness than in the longitudinal directions, due to the preferred in-plane macromolecular orientation induced by casting on glass. The degree of anisotropy when swollen in MA was found to be 7.8 : 1 and 1.4 : 1 for CA-2.45 and CA-2.0, respectively

(indicating significant loss of in-plane orientation upon hydrolysis, in line with a corresponding reduction in molecular weight from $\bar{M}_w$ = 142 to 55 K, based on light-scattering measurements of trifluoroethanol solutions[11] of the relevant polymers). MC and MA were of analytical reagent grade.

Methods

Rectangular (5×3 mm^2) film strips were clamped between two microscope slides with spring clips of known stiffness and immersed in a small trough containing liquid penetrant at room temperature (24 ± 1°C) (see Fig. 1). The spring clips were designed to apply pressure at one point on the upper plate and two points on the lower plate (as illustrated in Fig. 1 of Ref. 5) and metallic fillers ca. 10 μm thinner than the film specimen were inserted between the plates to prevent excessive squeezing of the specimen in cases where the latter became too soft to support the clamping pressure.

Optical Path Difference (OPD) Profiles

The penetration experiments were performed on the stage of a microscope (Amplival Pol U of Jena) equipped with a 40 mm objective and 12× eyepiece and set up for two-beam interferometry operating on the shearing principle. In this setup, a Mach-Zehnder interferometer produces two laterally displaced images of the specimen under examination traversed by parallel interference fringes. In our case, the fringes in the liquid region were aligned with the direction of penetration X' and their lateral displacement at any X' gave $\Delta y(X')$.[12] OPD profiles extending over penetration distances $X' < 0.4$ mm could be determined.

Swelling of the Clamped Specimen in the Thickness Direction

The change in thickness Δl could be detected either mechanically or optically. In the former method, the displacement of a nonmagnetic feeler resting on the upper glass plate and carrying the core of a sensitive inductive transducer (Schaevitz, type 0.50HR, sensitivity 2.2 mvolt/μm) was recorded, using the apparatus shown in Figure 2. Δl values as low as 0.05 μm were detectable. These values are expected to reflect changes in l_L (Δl_L) since the concentration of penetrant in the film attains the highest value (C_s) at $X' = 0$.

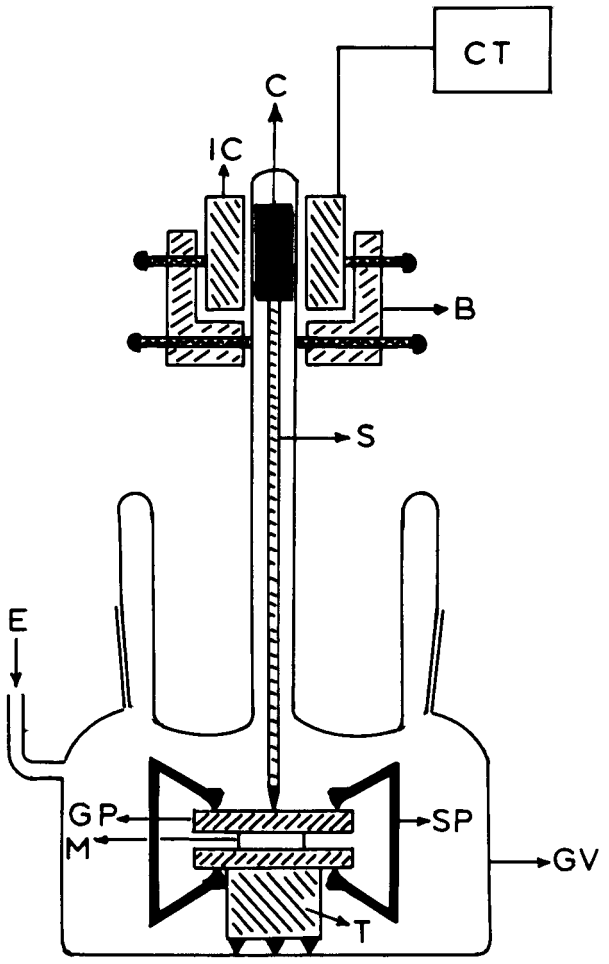

Figure 2 Setup for the mechanical measurement of the swelling of the clamped film specimen, during penetration experiments. GV: glass vessel, M: membrane, SP: spring clips, T: three legged base for support of the specimen, S: nonmagnetic feeler, IC: transducer induction coil, C: core of the transducer, B: base for the support of the transducer coil on the glass tube, E: inlet for the liquid penetrant, GP: glass plates, CT: control unit of transducer.

An optical method which is also specific for l_L involved rapid replacement of the liquid penetrant between the glass plates (by absorption on filter paper) with another immiscible liquid (dibutyl phthalate was used for this purpose) of a different refractive index n'_L. A new value for the OPD of the edge of the film specimen $\Delta y'(X' = 0)$ was then measured and l_L was deduced from

$$\Delta y'(X' = 0) - \Delta y(X' = 0) = l_L(n'_L - n_L) \quad (4)$$

On the other hand, the change of thickness of the dry part of the film Δl_0 could be measured by following the displacement δy_0 of a given fringe in this region from its original position using the relation

$$\delta y_0 = \Delta l_0(n_P - n_L) \quad (5)$$

Refractive Index–Concentration Relation

For the direct determination of the refractive index–concentration relation, clamped membrane specimens were placed in glass tubes, which were then connected to a vapor-sorption apparatus. In this case, beside the thin fillers normally used, additional thick fillers were inserted between the glass plates to ensure full exposure of the film specimen to the penetrant vapor. After evacuation, the specimens were equilibrated with different penetrant vapor pressures. In each case, a larger strip of the same membrane hanging from a quartz spring was used to determine (through the deflection of the quartz spring measured by a cathetometer) the equilibrium concentration of sorbed penetrant.[13] Then, the glass tube was opened to the atmosphere, the thick fillers quickly withdrawn, and the refractive index of the clamped specimen measured by the two-liquid microinterferometry technique described above. The preparation of specimens containing high penetrant concentrations was carried out in a chamber saturated with penetrant vapor to avoid significant evaporation of sorbed penetrant.

Penetration Kinetics and Birefringence Profiles

Supplementary measurements of penetration kinetics and strain birefringence were also carried out. For the former experiments, the microscope was set up with a 40 mm objective and a 10× graduated eyepiece. The position of the polymer–liquid interface at the commencement ($t = 0$) of the experiment was used as the origin ($X = 0$) for measuring the position X_P of visible inward-moving penetration fronts designated B ($X_{P\mathrm{B}} > 0$) and outward-moving swelling fronts designated A ($X_{P\mathrm{A}} < 0$), as a function of time t (see Fig. 1). Such visible penetration or swelling fronts, which appeared in the microscope field as straight lines normal to penetration axis, are manifestations of steep changes in $\partial n/\partial x = (\partial C/\partial x)(dn/dC)$ (i.e., large values of $\partial^2 n/\partial x^2$), which are, in turn, due to sharp changes in $\partial C/\partial x$ (sharp steepening of the concentration profile) and/or dn/dC (marked deviations from the linear n–C relation).

In the latter experiments, the appearance and variation of strain birefringence B_R along the axis of penetration could be recorded directly against a scale by setting up the microscope for polarized light with crossed nicols (polarizer and analyzer), a Wright eyepiece, and a graduated wedge compensator set at an angle of 45° to the crossed nicols and at right angles to the axis of penetration. A first-order red plate was also introduced at 45° to the crossed nicols with its slow axis of transmission perpendicular to that of the wedge compensator.[1] With this setup, positive (negative) birefringence indicated a tendency for preferred macromolecular orientation along the plane of the film in the direction parallel (perpendicular) to the penetration axis.

Effect of Clamping Pressure

In the case of the CA-2.0/MA system, the effect of clamping pressure on the behavior of the system was studied by the use of (a) bare glass plates under a relatively high clamping pressure (estimated compressive force 7.8 N), (b) glass plates smeared with a very thin film of silicone grease under the same clamping pressure as above, and (c) glass plates smeared with silicone grease under a relatively weak clamping pressure (estimated compressive force 4.4 N).

RESULTS AND DISCUSSION

Optical Path Difference (OPD) and Birefringence Profiles

The OPD and corresponding B_R profiles for the systems studied are shown in Figure 3. The CA-2.45/MC system [Fig. 3(a)] is distinguished by a highly swollen region characterized by small Δy values, which increase gradually (corresponding to high penetrant concentration decreasing gradually) with X' from the swelling front A up to a sharp visible penetration front B2. The latter marks a sharp rise in Δy corresponding to a sharp drop in C. The highly swollen polymer behaves essentially as a viscous liquid unable to sustain any strain birefringence (cf. the corresponding B_R profile). A meniscus is formed at the swelling film edge, as indicated by the steepening of the OPD

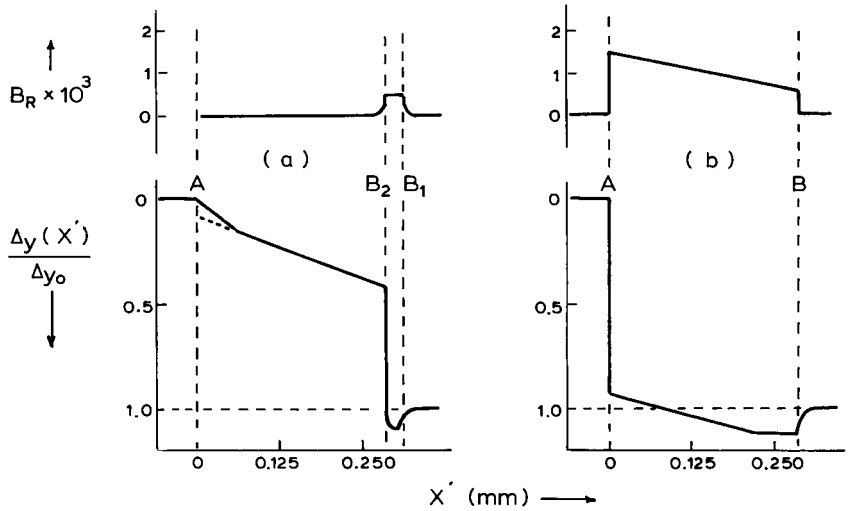

Figure 3 Relative optical path difference $[\Delta y(X')/\Delta y_0]$ and strain birefringence (B_R) profiles for penetration of (a) MC in CA-2.45 and (b) MA in CA-2.0.

profile near front A, which wipes out the expected discontinuity in OPD at the polymer–liquid interface (in keeping with the fact that MC is a strong swelling agent, but not a solvent, of CA-2.45 [Ref. 3]). Extrapolation of the less steep part of the profile to front A leads to such a discontinuity amounting to $\Delta y(X' = 0)/\Delta y_0 \sim 0.1$, which is in line with the swelling ratio of the free film reported in the Experimental section. Beyond front B2 (i.e., for $X' > X'_{B2}$), we have a weakly swollen region characterized by the occurrence of Δy values exceeding Δy_0, indicating that $n(C)$ at low C deviates markedly from linearity and passes through a maximum. The appearance of a faint penetration front B1 in this region is presumably attributable to the aforesaid sharp deviation of $n(C)$ from linearity (see below). Hence, to obtain even a qualitative picture of the concentration profile in this region (as well as an accurate quantitative picture of the high concentration profile), direct determination of the refractive index–concentration relation is necessary.

The situation in CA-2.0/MA is much the same, except that, in view of the fact that MA is a rather poor swelling agent of CA-2.0, there is no highly swollen region. The weakly swollen region extends to the swelling front A, where a large discontinuity in Δy is found, and includes a visible penetration front B similar to B1 in the case of CA-2.45/MC. These features were observed under all clamping conditions described in the preceding section.

Refractive Index–Concentration Relations

In view of the above findings, the refractive index–concentration relation for both systems was determined separately as described in the Experimental section. The results, shown in Figure 4, exhibit some variability, especially in the case of CA-2.45/MC [Fig. 4(a)]. In both cases, the n–C relation goes through a maximum in the low concentration region, in line with what can be expected when excess free volume is being filled (see Introduction) and with the observed behavior of the refractive index in other CA-penetrant systems.[3,9,14,15] It is noteworthy that measurement of a substantial portion of the n–C curve for CA-2.45/MC, using (i) films prepared from a different sample of CA powder and (ii) a different interferometric technique ("optical thickness meter" of Zeiss, Germany), gave results[16] in close agreement with Figure 4(a).

Penetration Rates

The kinetic plots describing the propagation of all observable fronts were found to be linear on a $t^{1/2}$ scale without any significant intercepts (except for front A in CA-2.0, see below), as illustrated by typical examples in Figure 5.

In the case of CA-2.45/MC, the swelling front A propagated outward at a rate comparable with that of B1, B2. In the case of CA-2.0/MA, however, the movement of front A was scarcely discernible

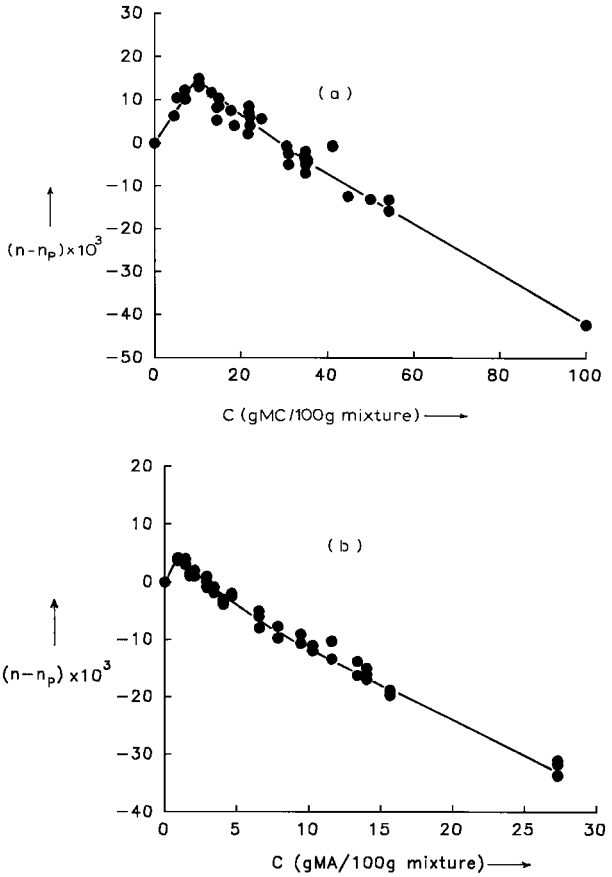

Figure 4 Dependence of the refractive index on penetrant concentration in the systems (a) CA-2.45/MC and (b) CA-2.0/MA.

under the higher clamping pressure, but became measurable when the glass plates were greased and was further enhanced when the clamping pressure was reduced. The mean measured rates of propagation were (in mm/min$^{1/2}$) (i) $dX_{PA}/dt^{1/2} = -0.131$, $dX_{PB2}/dt^{1/2} = 0.058$, and $dX_{PB1}/dt^{1/2} = 0.068$ for CA-2.45/MC and (ii) $dX_{PA}/dt^{1/2} = 0$, 0.0039, and 0.0047 and $dX_{PB}/dt^{1/2} = 0.0140$, 0.0130, and 0.0148 for higher clamping pressure, higher clamping pressure + greased plates, and low clamping pressure + greased plates, respectively, for CA-2.0/MA, showing that the rate of advance of front A increases significantly in this order, whereas the rate of propagation of front B is hardly affected (within experimental error).

Dilation in the Thickness Direction

Swelling of the clamped film specimen in the thickness direction was monitored by the methods described in the Experimental section. Typical results are shown in Figure 6.

For CA-2.45/MC, no detectable increase in specimen thickness over the original dry specimen value l_P was found [see Fig. 6(a)]. In the weakly swollen region of this system, a yield point is eventually attained, whereby the deficiency in thickness swelling can be made up by extra (plastic) dilation along the axis of penetration. The process is autocatalytic (the polymer becomes more strongly plasticized as more penetrant is taken up), with the result that equilibrium volume swelling is attained very fast, as indicated by the sharp drop in the OPD (reflecting a corresponding sharp rise in C) and simultaneous loss of birefringence (due to the fact that the preferred macromolecular orientation cannot survive in the highly plasticized polymer; v.s.), observed at front

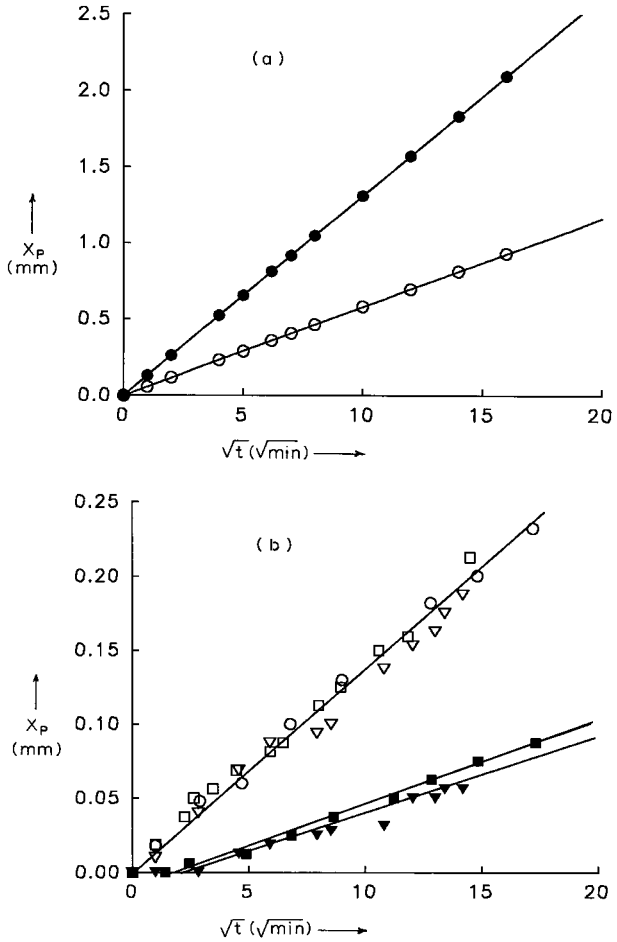

Figure 5 Typical examples of penetration kinetic experiments for the systems (a) CA-2.45/MC, (○) front B2, and (●) front A and (b) CA-2.0/MA, with higher clamping pressure + bare plates, (○) front B; higher clamping pressure + greased plates, (▽) front B and (▼) front A; and low clamping pressure + greased plates, (□) front B and (■) front A.

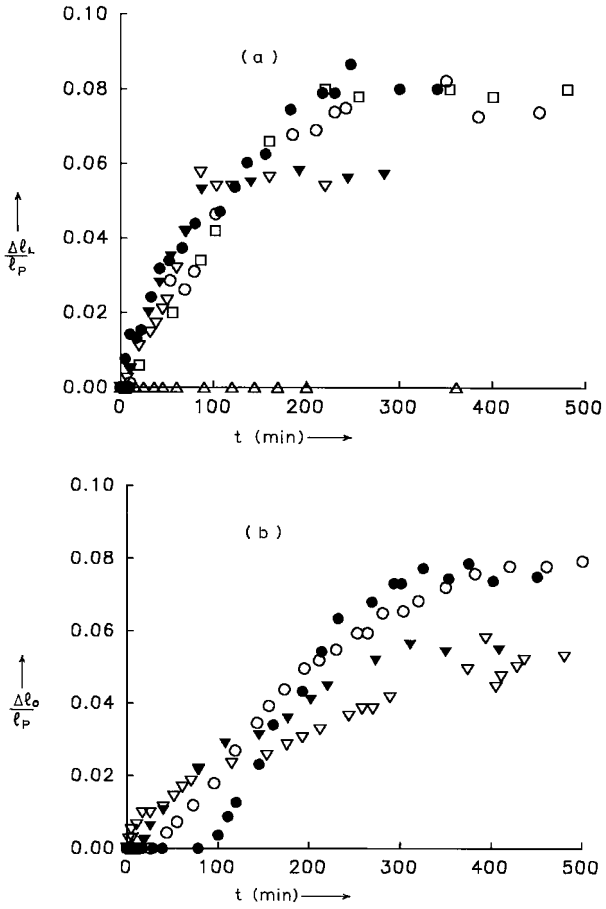

Figure 6 Typical examples of the fractional dilation of the clamped polymer film in the thickness direction, as a function of time. Results for (a) the swelling edge of the film ($\Delta l_L/l_P$) by the mechanical feeler method and (b) the dry film region ($\Delta l_0/l_P$), for the systems (△) CA-2.45/MC, (□) CA-2.0/MA with higher clamping pressure + bare plates, (○, ●) higher clamping pressure + greased plates, and (▽, ▼) low clamping pressure + greased plates.

B2. Note that, as a result of this behavior, the strained weakly swollen polymer region remains restricted between fronts B1 and B2. Thus, the force exercised on the glass plates by the swelling pressure of the polymer is correspondingly limited and is successfully resisted by the spring clips.

For CA-2.0/MA, on the other hand, the thickness of the clamped specimen increased with time, eventually attaining a plateau in all cases studied, as shown in Figure 6. As is also illustrated in Figure 6, the kinetics of dilation under given experimental conditions showed considerable variability, but the fractional dilation attained in the plateau region $\Delta l^c/l_P$ was quite reproducible. The results obtained under various conditions are given in Table I, where values of $\Delta l^c/l_P$ determined by the two-liquid method are also included. The latter values tend to be systematically higher than those obtained with the mechanical feeler and are expected to be less reliable (because of the possibility of systematic errors in $\Delta y'(X' = 0)$ arising from MA leaving, or dibutyl phthalate entering, the film, when the former is replaced by the latter), but they still provide a useful confirmation of the trend observed with changing experimental conditions. In particular, Table I shows that swelling in the thickness direction is reduced by greasing the glass plates and lowering the clamping pressure. As previously noted, longitudinal swelling in the $-X$ direction is enhanced by the above changes in conditions and calculation [for times corresponding to the plateau regions in Fig. 6(a)] shows that overall (volume) swelling in the A front region is also enhanced, indicating that, as expected, the penetrant concentration C_s at the front A approaches the equilibrium concentration C_0 (determined by immersing the free film in liquid MA) more closely, as the constraint upon swelling (namely, the clamping pressure primarily and friction between swelling polymer and glass plates secondarily) is lessened.

The B_R results reveal the buildup of strain along the penetration axis in the swelling polymer region, which is induced by the compressive stress suffered by the polymer, as a result of the constraint on swelling in the thickness direction (a similar constraint is imposed by the dry polymer in the other longitudinal direction). As the swelling region between the edge of film A and the visible penetration front at B increases in extent, the total swelling force in the thickness direction also increases and tends to push the glass plates

Table I Fractional Dilation (%) in the Thickness Direction in the Plateau Region, During Penetration of MA in CA-2.0 Film, Under Conditions of (a) High Clamping Pressure + Bare Plates, (b) High Clamping Pressure + Greased Plates, and (c) Weak Clamping Pressure + Greased Plates; (i) at Front A ($\Delta l_L^c/l_P$) by the Mechanical Feeler Method, (ii) at Front A by the Two-Liquid Optical Method, and (iii) in the Dry Film Region ($\Delta l_0^c/l_P$)

	(a)	(b)	(c)
(i) $\Delta l_L^c/l_P$	8.1	7.6	5.5
(ii) $\Delta l_L^c/l_P$	10.4	9.0	6.9
(iii) $\Delta l_0^c/l_P$	8.3	7.8	5.2

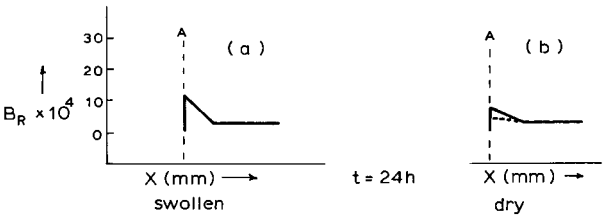

Figure 7 Typical birefringence, B_R, profiles of liquid methanol in CA-2.0 obtained upon (a) completion of penetration and (b) subsequent deswelling of the film specimen (results for higher and lower clamping pressure shown by full and dotted lines, respectively).

increasingly apart, until the plateau is attained. The B_R profile shows that the corresponding compressive stresses suffered by the swollen polymer tend to produce increasing strain in the outer swollen layers, which is partly plastic, because part of the strain birefringence persists after the film is fully penetrated and upon subsequent deswelling (see Fig. 7). Furthermore, Figure 7(b) shows that, as expected, the plastic deformation is higher under higher clamping pressure (thereby enabling C_s to approach C_0 more closely than would have been possible otherwise).

As far as the conversion of the experimental OPD profiles to the corresponding refractive index profiles is concerned, the salient feature of interest in the results reported in Figure 6(b) and in Table I is that the thickness of the dry region of the film specimen was also found to increase (presumably as a result of the resilience of the dry film, when the clamping pressure on it is relieved by the swelling part), albeit at a lower rate, especially when the clamping pressure is low [cf. Fig. 6(a) and (b)]. However, l_0 eventually attained very nearly the same plateau as that of l_L, thus ultimately eliminating any significant deviation from uniform specimen thickness, as shown in Table I. Thus, eq. (3b) is valid for CA-2.45/MC and is also applicable to CA-2.0/MA at reasonably long penetration times.

Penetrant Distribution Profiles

On the basis of the above findings and the refractive index–concentration relations of Figure 4, the OPD profiles of CA-2.45/MC and CA-2.0/MA were converted to the corresponding penetrant concentration profiles, illustrated in Figures 8 and 9, respectively.

In the case of CA-2.45/MC, good agreement between the values of C_s and C_0 was observed, as indicated earlier. This, in conjunction with a relatively fast relaxation process at the front B2,[5,6] sets the stage for a penetration process rate controlled by Fickian diffusion in the highly swollen region and, hence, obeying $t^{1/2}$ kinetics, as indicated by the penetration rate data. The shape of the diffuse precursor front ahead of B2 (the appearance of which accords with expectation based on model calculations[17]) is difficult to define with some precision, in view of the scatter of the experimental $n-C$ data, but the results of Figure 8 confirm that the B1 front appears as a result of a purely optical effect, bearing little relation to the concentration profile at that point, as suggested in previous articles.[5,6]

Penetrant concentration profiles of MA in CA-2.0 are given for different penetration times and conditions of constraint in Figure 9(a)–(c). Some discernible anomalies near the swelling front in Figure 9(c) may be due to anomalies in changes of thickness, which tend to be more pronounced at low clamping pressure, as previously indicated [see Fig. 6(a) and (b)]. Even so, the significantly closer approach of C_s to C_0 at the lower clamping pressure is clear and in close agreement with our previous calculations on the basis of data of thickness and longitudinal swelling. (Thus, e.g., for a penetration time of 400 min, values of C_s = 20 and 23 g MA/100 g mixture were calculated, as compared with C_0 = 27 g MA/100 g mixture, under conditions of higher clamping pressure + bare plates and lower clamping pressure + greased plates, respectively). The fact that front B (which corresponds to B1 in CA-2.45/MC) is a purely optical effect is also clearly demonstrated. The fact that no significant deviation from Fickian kinetics

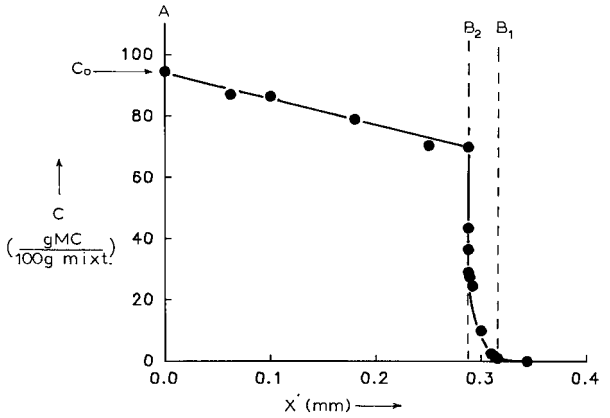

Figure 8 Concentration profile during penetration of MC in CA-2.45. The concentration C_0 of the free equilibrated specimen is indicated by the arrow.

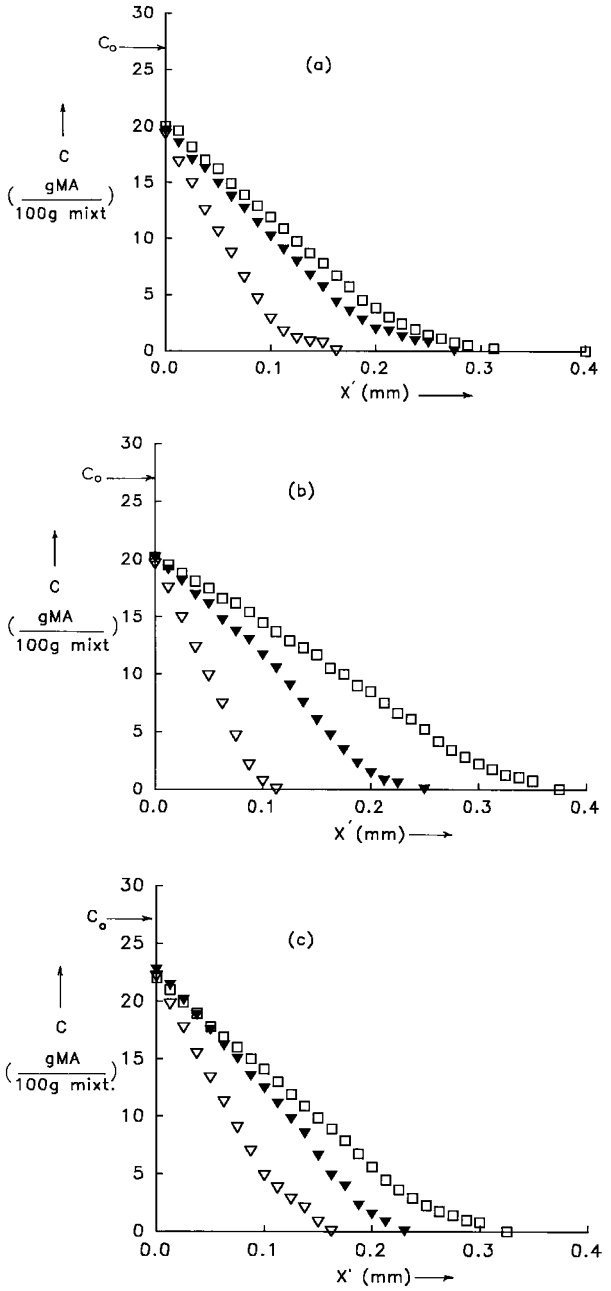

Figure 9 Concentration profiles at different times during penetration of MA in CA-2.0 with (a) higher clamping pressure + bare plates, t = (▽) 115 min, (▼) 330 min and (□) 581 min; and (b) higher clamping pressure + greased plates, t = (▽) 90 min, (▼) 183 min, (□) 444 min, and (c) low clamping pressure + greased plates t = (▽) 50 min, (▼) 150 min, and (□) 220 min. The concentration C_0 of the free equilibrated specimen is indicated by the arrow.

is discernible in the penetration rate data implies coincidence of the concentration profiles when plotted as C/C_s vs. $X'/2t^{1/2}$, which can serve as a useful criterion that the said profiles must fulfill if correctly determined. The combination of high clamping pressure and low frictional resistance seems to be most conducive to precision in the determination of concentration profiles and Figure 10 shows excellent coincidence of the profiles of Figure 9(b) for different times, when plotted in the aforementioned way.

CONCLUSION

Some phenomena relating to liquid penetration along nonrigidly clamped stiff-chain polymer films, which should be taken into account for the proper conversion of interferometric data to penetrant concentration profiles, have been investigated, with particular reference to (i) marked deviations of the refractive index–concentration relation from linearity in the low-concentration region and (ii) swelling of the clamped film specimen in the thickness direction. The conversion of OPD, to penetrant concentration, profiles is reported for the systems CA-2.45/MC and CA-2.0/MA, exemplifying the cases of strong and relatively weak swelling agents, respectively.

Effect (i) was important in both cases, necessitating direct determination of the refractive index–concentration relation. The results confirmed our previous conclusions regarding the nature of the diffuse penetrant profile preceding the sharp penetration front B2 observed in CA-2.45/MC, including the suggestion that the visible

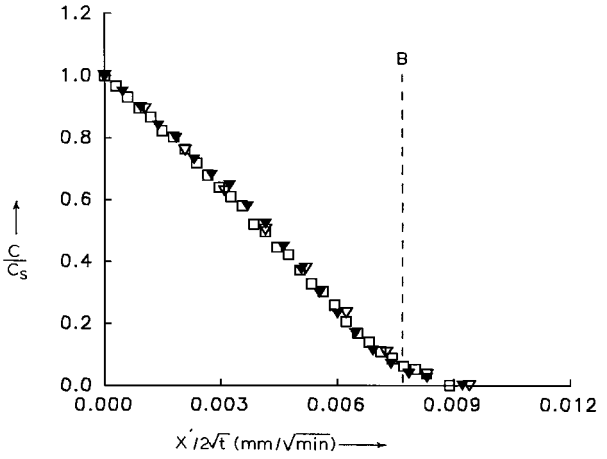

Figure 10 Normalized concentration profiles (C/C_s) vs $X'/2\sqrt{t}$) at different times during penetration of MA in CA-2.0 with higher clamping pressure + greased plates, t = (▽) 90 min, (▼) 183 min, and (□) 444 min.

front B1 as well as front B observed in CA-2.0/MA are purely optical effects.

Effect (ii) was observed in CA-2.0/MA but not in CA-2.45/MC. The relevant birefringence profiles indicate that, as the polymer begins to swell, considerable strain in the direction of penetration develops, as a result of stresses generated by the constraint imposed on swelling in the lateral directions (as shown here, frictional resistance to dilation in the $-X$ direction also contributes significantly to the aforementioned constraint). In the case of CA-2.45/MC, the polymer soon becomes sufficiently plasticized to deform plastically in the $-X$ direction, thus relieving the stress and at the same time limiting the force exercised by the swelling pressure of the polymer on the confining glass plates.

In the case of CA-2.0/MA, however, stress relaxation in the above way can occur only to a limited extent, and as the swelling region of the film continues to increase in extent, a sufficient swelling force develops to push the glass plates increasingly apart. The data obtained here show that the plateau which is eventually reached depends on clamping pressure but is otherwise quite reproducible. Furthermore, at least at moderate degrees of dilation, the thickness of the dry polymer region, measured optically, tends to change similarly. Thus, under appropriate conditions, the thickness of the specimen remains essentially uniform and conversion of the OPD to the concentration profile presents no greater difficulty than in the case of CA-2.45/MC.

The resulting concentration profiles depend to some extent on clamping conditions, the main effect being a closer approach of the concentration C_s at the swelling front A to the equilibrium value C_0, under conditions of low clamping pressure and frictional resistance. On the other hand, a higher clamping pressure appears to be more conducive to precise results.

REFERENCES

1. C. Robinson, *Trans. Faraday Soc.,* **42B,** 12 (1946).
2. G. S. Hartley, *Trans. Faraday Soc.,* **45,** 820 (1949).
3. C. Robinson, *Proc. R. Soc. Lond. A,* **204,** 339 (1950).
4. J. Crank and C. Robinson, *Proc. R. Soc. Lond. A,* **204,** 549 (1951).
5. M. Sanopoulou and J. H. Petropoulos, *J. Polym. Sci. Polym. Phys. Ed.,* **30,** 971 (1992).
6. M. Sanopoulou and J. H. Petropoulos, *J. Polym. Sci. Polym. Phys. Ed.,* **30,** 983 (1992).
7. T. G. Scholte, *J. Polym. Sci. A2,* **10,** 519 (1972).
8. E. F. Gurnee, *J. Polym. Sci. A2,* **5,** 799 (1967).
9. D. P. Malladi, J. R. Scherer, S. Kint, and G. F. Bailey, *J. Membr. Sci.,* **19,** 209 (1984).
10. E. D. Klug, in *Cellulose and Cellulose Derivatives,* 2nd ed., Part III, Vol. V, *High Polymers,* E. Ott, H. M. Spurlin and M. W. Grafflin, Eds., Interscience, New York, 1955, p. 1397.
11. D. W. Tanner and G. C. Berry, *J. Polym. Sci. Polym. Phys.,* **12,** 941 (1974).
12. G. Guerra, A. Moschetti, C. Carfagna, U. Mandara, A. Cutolo, and S. Solimeno, *J. Appl. Polym. Sci.,* **29,** 2271 (1984).
13. D. F. Stamatialis, PhD Thesis, University of Athens, 1995.
14. J. R. Scherer and G. F. Bailey, *J. Membr. Sci.,* **13,** 29 (1982).
15. B. A. Bolton, S. Kint, G. F. Bailey, and J. R. Scherer, *J. Phys. Chem.,* **90,** 1207 (1986).
16. D. F. Stamatialis, M. Wessling, M. Sanopoulou, H. Strathmann, and J. H. Petropoulos, to appear in *J. Membr. Sci.*
17. J. H. Petropoulos and M. Sanopoulou, *J. Polym. Sci. Part B Polym. Phys. Ed.,* **26,** 1087 (1988).